

合成燃料优化及提升发动机效率的实验与仿真研究

VILLFORTH Jonas¹, CASAL Kulzer André¹, ROSSI Edoardo², VACCA Antonino², CUPO Francesco², CHIODI Marco², BARGENDE Michael³

(1. Dr. Ing. h.c. F. Porsche AG, 魏斯阿赫 71287, 德国; 2. 斯图加特内燃机与车辆研究所, 斯图加特 70569, 德国;
3. 斯图加特大学 车辆工程与发动机学院, 斯图加特 70569, 德国)

摘要: 减少二氧化碳排放, 特别是减少汽油发动机的二氧化碳排放是目前正在急剧上升的一项要求。从能源的生命周期考虑, 能源载体即化石燃料是产生二氧化碳排放问题的根本原因。采用从可再生能源中提炼出的合成燃料(eFuel), 可使汽油发动机接近或达到二氧化碳排放的碳中和要求, 因此配置 eFuel 的成分和性质至关重要, 因为它将影响汽油发动机的工作过程和效率。eFuel 的成分变化会显著影响汽油发动机的喷射、混合气形成、燃烧, 以及后氧化和排气后处理等过程, 因此, Dr. Ing. h.c. F. Porsche AG 和 FKFS 合作开展了一系列相关研究, 将不同的 eFuel 在单缸发动机试验台和喷雾试验台上进行了测试, 并将其结果用于标定三维流体的仿真模型。同时, 对 eFuel 的组成、混合气形成及燃烧特性进行深入分析, 旨在提高汽油发动机效率, 同时改善碳排放效果。除了进行单缸发动机测试外, 还对汽油发动机配置进行虚拟优化, 即通过替代燃料与发动机优化的相结合来提升汽油发动机的效率。

关键词: 汽油发动机; 合成燃料; 二氧化碳减排; 发动机效率
中图分类号: U473 **文献标志码:** A

Experimental and Numerical Identification and Optimization of eFuel Potentials on Combustion Behavior and Engine Efficiency

VILLFORTH Jonas¹, CASAL Kulzer André¹, ROSSI Edoardo², VACCA Antonino², CUPO Francesco², CHIODI Marco², BARGENDE Michael³

(1. Dr. Ing. h.c. F. Porsche AG, 71287 Weissach, Germany; 2. FKFS, 70569 Stuttgart, Germany; 3. Universität Stuttgart, 70569, Germany)

Abstract: The demand for CO₂ reduction is rising sharply nowadays, especially for gasoline engines. Considering a life cycle analysis, the energy carrier, i.e. the fossil fuel is responsible for the emissions problem. The defossilization towards synthetic fuels from renewable energy sources

(eFuels), can make the combustion engine almost CO₂ neutral. The design of an eFuel composition and properties is crucial, as its formulation influences the gasoline engine processes and efficiency. From injection, mixture formation and combustion to post-oxidation and exhaust after treatment, a change in fuel composition has significant effects. For these reasons, several research projects were conducted as part of a collaboration between Dr. Ing. h. c. F. Porsche AG and FKFS. Measurements of a single-cylinder engine test bench and of a spray test ring with different fuels were produced and used to calibrate 3D-CFD simulation models. The fuel formulation, mixture formation and combustion behavior were analyzed deeply, with the aim of increasing engine efficiency while improving emissions. A virtual optimization of the engine configuration was possible in addition to single-cylinder engine tests, leading to significant potentials through alternative fuels and engine optimization.

Key words: gasoline engine; eFuel; CO₂ reduction; engine efficiency

1 Introduction

In order to achieve the ambitious goals of the Paris Climate Agreement^[1], the transformation of the transport sector to electromobility is far from sufficient. A transformation of the energy sources used rather than a transformation of powertrain technology is required. Electricity-based fuels (eFuels) are a considerable contribution to reach the ambitious goals. The use of eFuels can significantly

improve the CO₂ footprint of existing vehicles with conventional combustion engines by balancing the CO₂ cycle across sectors. Given the large number of vehicles in the fleet, this is a promising opportunity to contribute to defossilization and CO₂ reduction within the transport sector.

In addition to the almost neutral CO₂ cycle, eFuels offer additional degrees of freedom in the formulation and therefore the associated properties. The fuel as a further development and optimization parameter can enable previously unused possibilities for engine combustion. For the application in the existing vehicle fleet, the emissions and their reduction potentials via eFuels are the main focus. The fuel-related changes in emission behavior have been reported in several publications^[2-4]. Kulzer et al. has already discussed advantages in anti-knock properties and the associated reduction in the center of combustion. In addition to improved engine roughness, this also leads to increased efficiency with the same engine configuration^[3].

In the present work, possibilities for increasing efficiency through optimized engine geometry and combustion processes are investigated. Three engine configurations are compared experimentally with respect to combustion quality, efficiency and emissions. In addition to the effects of engine optimization, further improvements via the used fuel formulation are highlighted. As part of the research project, FKFS supported the single-cylinder engine investigation and the fuel development through the 3D-CFD (computational fluid dynamics) analysis of the engine flow field, the combustion process and the injectors behavior. After the calibration of the 3D-CFD simulations through the optical experiments led at FKFS and the measurements at the single cylinder engine carried out at Dr. Ing. h. c. F. Porsche AG, the virtual development focused on the optimization of the fuel evaporation and the knock resistance.

The developed simulation and analysis methods allow an efficient and fast evaluation of potentials in the combustion process in combination with the fuel formulation to optimize combustion and efficiency.

2 Research objects and methods

In order to increase the efficiency of the internal combustion engine, various configurations of a Porsche research single-cylinder engine (SCE) were investigated as part of this work. The focus here was on the application of basic approaches to increasing engine efficiency. In addition to the experimental investigations, methods were developed for evaluating engine and fuel-specific influences on efficiency. For this purpose, 3D-CFD simulations were calibrated and validated using experimental data. Assessment approaches were developed for an in-depth understanding of the mechanisms and influences on combustion.

2.1 Experimental setup and tested fuels

The experimental evaluation of the efficiency potential was conducted on three configurations of the Porsche research single cylinder engine (see Fig. 1). Starting from the basic configuration, which has already been described in detail in previous publications^[3-5], a more advanced combustion process with a piezo actuated hollow cone nozzle (HCN) was used. In the course of the improved cylinder head geometry, the piston was also adapted to raise the compression ratio from 12.5 to 13.0. Both stroke and bore were kept constant. As a complementary method for possible efficiency increase, intake and exhaust camshafts come with the possibility to represent a Miller-cycle.

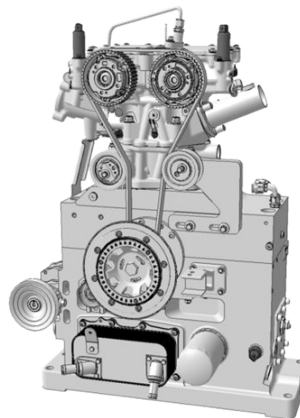


Fig. 1 CAD illustration of the Porsche research SCE

In addition to the hardware configuration with a constant stroke/bore ratio, a variant with a reduced bore diameter was built. Here, only the bore was reduced, and the combustion chamber geometry scaled accordingly. The background to this is to use the increase in the stroke/bore ratio and the associated influences on the combustion chamber geometry (surface/volume ratio, quench areas) for optimized combustion. From 3D-CFD considerations, it has been shown that improved mixture formation can be achieved with a multi-hole nozzle (MHN) especially when using Porsche Synthetic fuel (POSYN)^[6]. A multi-hole injector was therefore used for the engine variant with reduced bore diameter. To further investigate combustion design potentials a passive

prechamber spark plug (PCSP) was used with the small-bore engine. As the design of the PCSP (hole geometry and orientation, volume, ...) has a decisive influence on the combustion performance, a specific design of the PCSP in combination with the engine geometry and combustion design is essential to exploit the maximum potential. For the present investigations a non-optimized prechamber geometry was used to initially identify the influence of a PCSP on the combustion of the existing engine configuration.

All three engines were calibrated using the RON98 base fuel. The main engine parameters for all three investigated single cylinder engines are given in Tab. 1.

Tab. 1 SCE engine specifications

Engine specifications	Cubic capacity/cm ³	Bore/mm	Stroke/mm	Stroke/Bore	Compression ratio	Number of valves	Injector	Injection pressure/bar	Ignition
Base setup	598.6	97.0	81.0	0.835	12.5:1.0	4	HCN	200	Conv. SP
High Eps	598.6	97.0	81.0	0.835	13.0:1.0	4	HCN	200	Conv. SP
Stroke / Bore	498.3	88.5	81.0	0.915	13.2:1.0	4	MHN	350	Conv. SP / PCSP

2.2 Investigated fuels and test procedure

In addition to the experimental evaluation of the influence of engine geometry and combustion process on combustion and efficiency, fuel-related effects are also discussed in this paper. No changes were made to the engine calibration for the fuel investigations. The identified potentials can be expanded and exploited via a fuel-specific calibration.

The RON 98 fuel, which was also used for the base calibration, serves as a reference. In order to increase the efficiency through the fuel, two fuels were selected which, with an increased octane number, contribute to a reduction of center of

combustion (50% mass fraction burned (MFB 50)) at high load. For this purpose, a POSYN fuel and an E 10 racing fuel were used. In addition to increased anti-knock properties, the POSYN is specified for improved emission formation. Some of the potentials regarding emissions, post oxidation and mixture formation potentials using a Porsche synthetic fuel formulation were discussed in previous publications^[3-6]. This is achieved by an advanced fuel formulation. In addition, optimized evaporation behavior leads to rapid evaporation and consequently to an influence on mixture formation. The main fuel properties are listed in Tab. 2.

Tab. 2 Fuel properties of tested fuels on SCEs

Fuel properties	Oxygenates/vol%	Olefins/vol%	Aromatics/vol%	Saturates/vol%	RON	MON	C/H ratio	C/O ratio	LHV/(MJ/kg)	A/F ratio	Final boiling point/°C
RON 98	0.3	6.0	25.5	56.1	98.4	88.0	1.973	0.018	42.16	14.21	196.3
POSYN	15.0	0.5	0.3	84.2	99.9	90.3	1.873	0.023	42.92	14.50	147.8
Racing fuel	10.1	13.6	33.3	42.7	100.4	89.3	1.753	0.032	41.09	13.74	159.8

Three representative operating points are considered out of engine map measurements for the evaluation with regard to combustion and engine efficiency. In order to take advantage of the increased

knock resistance of the fuels, the operating points are in the knock-limited range of the RON 98 map. In addition to low-end torque and rated power, operation at 4 000 r/min and increased load (14 bar BMEP) is

analyzed. Fig. 2 shows the map range of the RON 98 with conventional (solid black line) and pre-chamber spark plug (dashed grey). Next to the operating points for the evaluation, the knock-limited range (MFB 50 > 10° CA a. FTDC) is marked in green.

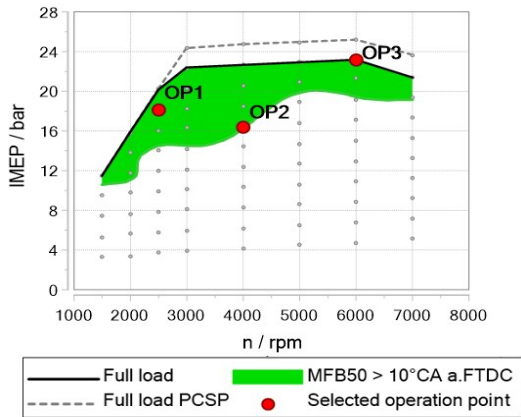


Fig.2 Overview of engine map operation range and investigated operation points

With the aid of experimental investigations, potentials can be identified and, with the appropriate effort, optimization of the combustion process and fuel formulation can be performed. The large number of influencing factors makes this process very cost consuming and complex. It is therefore necessary to co-optimize the combustion design and fuel formulation using simulation methods.

2.3 Methodology for engine simulations regarding eFuel potentials

The numerical analysis presented in this paper was performed by means of 3D-CFD engine simulations with the simulation tool QuickSim, whose goal and methodology are described in detail in reference [7]. QuickSim is a fast response 3D-CFD tool developed and continuously improved at FKFS and IFS University of Stuttgart and it relies on the commercial software Star-CD as a solver, which allows the adoption of user models specifically designed for ICE simulations, such as injection, fuel and combustion models. The adoption of ICE-specific models and the optimization of the engine discretization, makes it possible to use coarser meshes with respect to traditional 3D-CFD approaches, thus leading to a significant reduction in

the computational time (one engine operating cycle of a full engine can be simulated in 2 hours using a 12-cores CPU), while maintaining high-quality simulation results.

Further advantage of QuickSim is the possibility to extend the computational domain, including the whole intake and exhaust systems. Fig. 3 shows the computational mesh adopted in the investigations reported in this work, which contains approximately 320 000 cells and it is a faithful reproduction of the complete test bench at which experiments have been conducted. The extension of the computational domain makes it possible to simulate several consecutive engine operating cycles, while limiting the influence of initial and boundary conditions, thus operating as a virtual test bench.

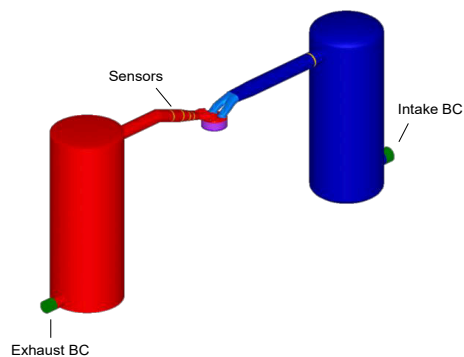


Fig 3 Single cylinder engine test bench model for 3D-CFD simulations

The specifications of the engine reproduced in the virtual test bench of QuickSim are reported in Tab. 1 as the base setup.

This model has been used for understanding the influence of the properties of the investigated fuel on injection, mixture formation, combustion characteristics and the overall efficiency of the engine. In the context of these kinds of analysis, a crucial aspect is found in the precise definition of the investigated fuel in the simulation environment, considering both its physical and thermodynamic properties. Furthermore, a reliable injection model has been implemented in QuickSim, whose validation and calibration were conducted by means of data collected during an experimental spray investigation of the considered fuels, including Phase Doppler

Anemometry and Mie scattering measurements, led in the optical laboratory of FKFS.

2.3.1 Fuel model description

The correct reproduction of the fuel characteristics in the simulation environment is fundamental, as the fuel properties, such as laminar flame speed and resistance to auto-ignition, directly reflect on the overall engine combustion behavior. Being the goal of QuickSim to achieve fast and reliable engine simulations, fuel modelling represent a preliminary step. Fuel modelling includes the formulation of a suitable fuel surrogate, which must take into consideration the actual fuel chemical composition, the definition of the fuel physical properties and the calculation of apposite look-up tables for properties such as laminar flame speed and auto-ignition delay under a variety of operating conditions, typical of ICE operations.

For a detailed description of the implementation of the fuel modelling in the 3D-CFD simulations with QuickSim, please refer to reference [8].

Regarding the choice and the definition of the fuel surrogate for the two investigated fuels, SP 98 and POSYN, a more complex formulation with respect to commonly used PRF (primary reference fuel) or TRF (toluene reference fuel) has been chosen, which includes at least one chemical species for each relevant chemical family present in the fuel formulation, i. e. n-Paraffins, Iso-Paraffins, naptenes, oxygenates and aromatics. Tab. 4 report the composition of the defined fuel surrogates for SP 98 and POSYN.

Tab. 4 Fuel surrogates composition for SP 98 and POSYN

Fuel properties	n and iso-Paraffins/Vol%	Naptenes/Vol%	Oxygenates/Vol%	Aromatics/Vol%
SP 98	41.55	2.62	11.74	34.11
POSYN	55.82	29.94	14.24	0

Chemical laboratory analysis provided experimental values for the fuels liquid properties, such as density, viscosity, surface tension, vapor pressure, specific heat capacity and heat of vaporization, which are then arranged into a look-up table as a function of temperature, and will be directly read during the 3D-CFD simulation.

One of the most crucial aspects in the

investigation of the engine combustion and knock tendency with different fuels is the modelling of laminar flame speed and auto-ignition delay. These properties are preliminary evaluated using detailed chemical kinetics calculations performed with a tool developed in Cantera, considering a wide range of lambda, temperature, pressure, residual gas rate and composition which are characteristic of typical engine operating conditions. The adopted chemical mechanism for the calculation of laminar flame speed and auto-ignition delay is the Lawrence Livermore National Laboratory (LVLL), that include 324 species and 5739 reactions, and it has been extensively validated^[9]. Such calculation is extremely demanding in terms of computational time, therefore not being worth of directly apply the chemical reaction mechanism in the 3D-CFD simulations. Instead, the detailed chemical reactions solved by Cantera are exploited to generate look-up tables for the simulation, which are able to keep low the computational time and improve the accuracy of the combustion process.

A comparison of laminar flame speed and ignition delay time for SP 98 and POSYN is reported in Fig. 4 and Fig. 5. POSYN (blue) presents higher laminar flame speed with respect to SP 98 (black), but comparable ignition delay time. It is worth mentioning, that the validation of this calculations has been performed comparing the pressure traces obtained at the test bench and from the 3D-CFD simulations, as no experimental data are available in such pressure and temperature ranges (a rapid compression machine could be used for validation, but at limited temperature and pressure values with respect to ICE typical thermodynamics).

The evaluation of knock in the 3D-CFD environment of QuickSim is based on the detailed reproduction of the fuel characteristics. Considering the fuel composition and the equivalent surrogate the specific fuel resistance to autoignition can be calculated through chemical mechanism. On the other side, this parameter can be used to evaluate the fuel tendency to autoignition before the spark plug triggers the combustion event. The auto ignition delay

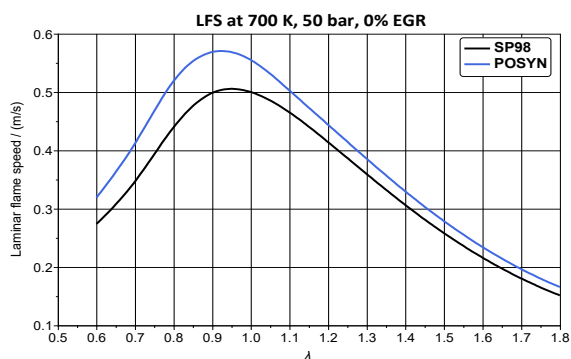


Fig.4 Laminar flame speed: 700 K, 50 bar, 0% EGR^[6]

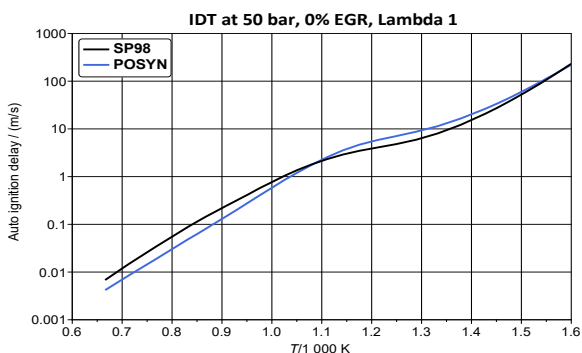


Fig.5 Ignition delay time: 50 bar, 0% EGR, $\lambda=1$ ^[6]

reported in Fig. 4, is the parameter that drives the optimization of the engine geometry with respect to the desired combustion design. In addition to the chemical description of the fuel through the laminar flame speed and the autoignition time, the 3D-CFD-Tool QuickSim links the knock onset with the engine thermo-fluid dynamics (flow field characteristics). Particularly the evaluation of knock considers the parameters such as the temperature of unburned gas, the residual gas content and its composition (reactive or inert), the local air to fuel mixture (λ), and the charge motion, in addition to the fuel composition.

These parameters are taken into account together considering their spatial and time evolution (as knock integral). With reference again to Fig. 4, the auto ignition characteristic of the fuels are calculated considering a full homogeneous reactor in Cantera, meaning that both the fuels are completely vaporized. One crucial aspect for the fuel development is of course that the evaporation behavior is taken into account. Therefore, QuickSim considers the fuel evaporation, based on a single-

component approach model, which is on the other side, tuned up by the pressure of saturation curve, experimentally measured for each fuel. It was found that such an approach was completely able to reproduce the different fuel behavior^[5-6].

2.3.2 Injection model description

Fuel spray propagation inside the combustion chamber and fuel evaporation have a significant impact on air-fuel mixture formation, hence on combustion behavior in an internal combustion engine. Therefore, it is necessary in the 3D-CFD simulations to reproduce in the most accurate way possible the fuel injection event.

The thorough description of the injection model implemented in QuickSim can be found in references [7] and [10], and the complete process of validation and calibration of the injection model by means of experimental data is reported in references [5] and [11].

The injection model in QuickSim presents some simplifications, in order to maintain the shortest computational time possible for the 3D-CFD simulations. For example, complex phenomena like the internal nozzle flow and the primary breakup are not simulated.

The injector geometry is not physically introduced in the computational mesh, instead the position of the injector is defined by means of a coordinate system accordingly positioned to match the z -axis with the main injector axis. Injector properties, such as mass flow rate, hydraulic delay, opening and closing time are defined in the settings of the simulation.

The injector considered in the numerical investigation is a piezo-actuated hollow-cone injector whose characteristics are summarized in Tab. 1. For this type of injector, the spray targeting is defined by means of an outer spray cone angle, the width of the injected hollow-cone, and the data that are provided by the injector manufacturer in the datasheet.

Particularly important for the correct reproduction of the spray propagation and fuel evaporation is the definition of the initialization conditions for the injection. The injected droplets are

Tab.5 Injector characteristics

Injector description	HCN (hollow-cone nozzle)
Max rail pressure	200 bar
Spray geometry	Symmetric hollow-cone, for central installation
Actuation	Piezo, directly coupled

initialized in a predefined region downstream the injector nozzle, and they are assigned with physical properties of the fuel, with values of temperature, size and velocity, according to the injection conditions. The size of the injected droplets is expressed in terms of SMD: a reference value is provided, and the injected droplets size follow a Rosin-Rammler distribution.

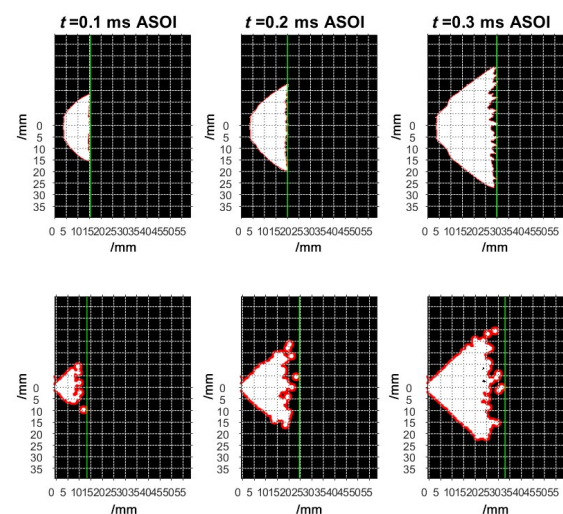
Within this study, an experimental spray investigation in a constant volume chamber has been conducted in order to validate and calibrate the numerical injection model. The complete calibration process is described in reference [6]. High-speed video analysis provided data about the main spray geometrical feature in time, i. e. spray axial and radial penetration, spray angle, and propagation speed under a variety of injection conditions, including variations in injection pressure and temperature, and chamber pressure. Furthermore, PDA measurements provided data about droplets size (SMD) and velocity, which made the characterization of the spray for different injection conditions possible.

Fig. 6 shows an example of a comparison between post-processed experimental high-speed video and a 3D-CFD simulation. In this example, an injection of POSYN with the hollow-cone injector is performed at 200 bar, with an injection duration of 0.3 ms, an injection temperature of 50 °C and a chamber pressure of 1 bar. The different frames correspond to different time instants, thus allowing a direct evaluation of the spray propagation produced by the simulation, in terms of spray axial and radial penetration and spray angle.

The optimization of the initialization parameters, alongside a tuning of some physical models, such as the droplets secondary breakup model, made it possible to obtain satisfactory results in terms of spray geometry and propagation reproduction, with a

maximum registered error in axial spray penetration at the end of injection below 10%.

A further step in the validation process of the injection model was the analysis of the droplets size and spray SMD, reproducing the PDA measurement process in the simulation environment. For both SP 98 and POSYN the registered droplets dimensions from the simulation were comparable with the measurement.



Hollow-cone injector, POSYN, injection pressure 200 bar, injection duration 0.3 ms.

Fig.6 Example of comparison between frames of experimental video (top row) and 3D-CFD simulation (bottom row) at different time instants

The process of calibration of the injection model also made it possible to prove the validity of the evaporation model adopted in the 3D-CFD simulations. The approach followed regarding the fuel evaporation in QuickSim is a single-component surrogate approach^[10]. This approach does not consider a boiling curve which accounts for the variations in fuel composition during the evaporation process due to the different volatility and boiling point of the different fuel components. Instead, the evaporation behavior is modeled by means of a precise calibration of the saturation pressure curve, which considers the partial pressures of the single components of the fuel and is validated exploiting the experimental data coming from a laboratory fuel analysis. This approach makes it possible to obtain a

realistic reproduction of the evaporation behavior of the fuel, without the great computational effort required by complete chemical analysis in multi-components fuel models.

3 Results and discussion

In this section different results are listed following the measurements led at the single cylinder test bench and the respective numerical analysis.

3.1 Influence of compression ratio and advanced combustion design

For the following consideration, the 50% mass fraction burned, the combustion duration and the average peak pressure are compared. As additional characteristics for the combustion quality, the engine roughness and the standard deviation of the peak pressure are important indicators. As a result of the improved combustion quality, the indicated efficiency is used. As already mentioned, emissions from combustion are always in the focus of interest. Therefore, also in the context of improved combustion and efficiency improvement, pollutants have to be kept in mind. For the experimental results, only the standard components (CO, THC, NO_x, PN, PM) are considered.

Fig. 7 shows the comparison of the three engine configurations at operating points OP1-OP3 in terms of combustion quality and efficiency. For the 50% mass fraction burned, OP1 shows no improvement and OP2 even shows a slight deterioration. Operation in low end torque is very sensitive to the charge motion. The selected camshafts are not optimized for this operation with the design in the direction of Miller timing. Despite this, combustion stability has been improved here. The main advantage comes at the high-load point (OP3). The MFB 50 could be reduced by more than 5° CA. In addition, the cycle variation was significantly improved. This is also reflected in the lower fluctuation of the peak pressure, which has improved at all three operating points. The faster combustion resulting from the optimized combustion process leads to an increased

average peak pressure, which is not a mechanical problem with a conventional spark plug.

The improved combustion characteristics of the optimized configurations ultimately lead to a significant increase in the indicated efficiency. The improvement in OP3 is particularly large. However, increasing the stroke/bore ratio did improve the indicated efficiency compared to the setup with increased compression ratio and advanced combustion design. Another influencing factor besides the improved stroke to bore ratio, is the multi-hole nozzle which was used with regard to the use of advanced eFuel formulations based on the simulation study reported by Rossi et al. [6].

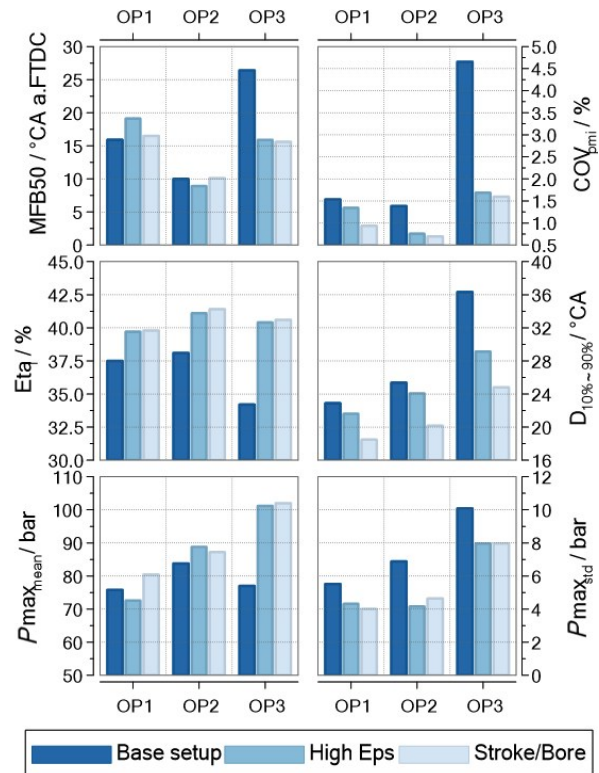


Fig. 7 Influence of engine configuration for investigated operation points regarding combustion and engine efficiency

In addition to the positive effects on combustion behavior, gaseous emissions were basically kept at the level of the basic setup. As Fig. 8 shows, CO and THC emissions were reduced across the board except for OP3. Due to the formation mechanism of the nitrogen oxides, the influences of the engine configurations in the center of combustion and peak

pressure are directly reflected in the NO_x emissions. In essence, optimized charge motion improved mixture formation and thus achieved a significant reduction in particulate emissions, especially for OP3.

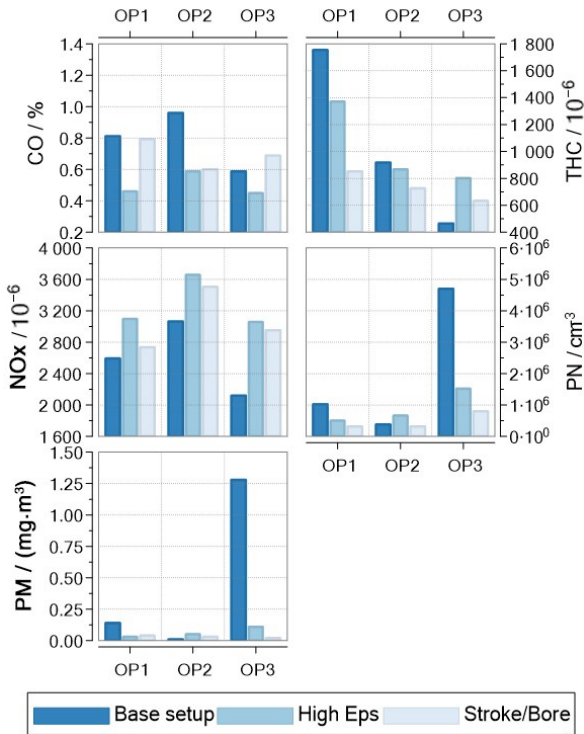


Fig.8 Influence of engine configuration for investigated operation points regarding emissions

3.2 Passive pre-chamber combustion

To further increase combustion quality and engine efficiency a passive prechamber spark plug was used. In addition, advanced fuel formulations were tested for increased engine efficiency due to high RON. Fig. 9 shows the experimental results for the different fuels with the conventional spark plug and a passive PCSP in the small-bore diameter setup.

For the RON 98 reference fuel the center of combustion could be significantly reduced using the PCSP. The combustion duration and coefficient of variance can be improved using a prechamber spark plug. For the present experimental investigations this behavior could be observed. The short burn duration induced by the jets of the prechamber leads to an increased mean peak pressure but with low standard deviation which is another indication of the stability of the combustion (see Fig. 10).

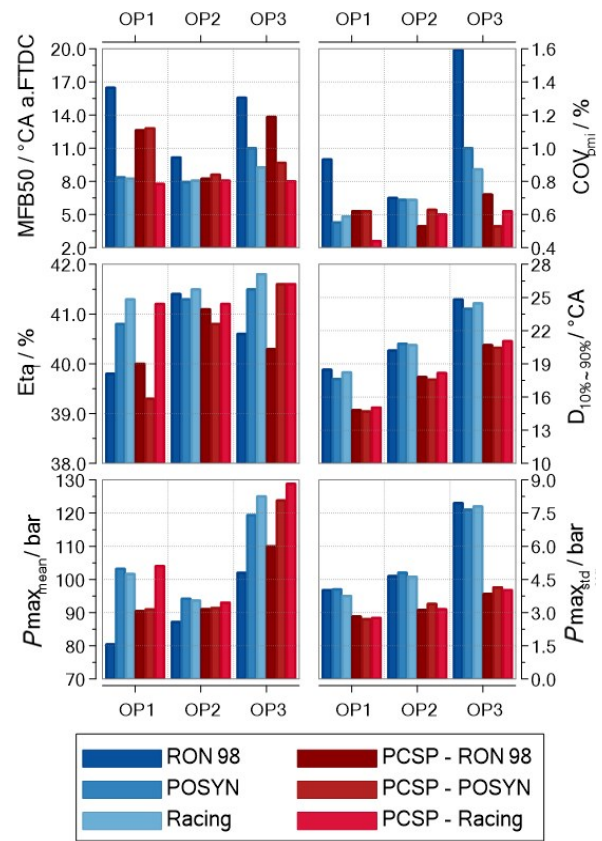


Fig.9 Influence of fuel and passive prechamber ignition on combustion and engine efficiency

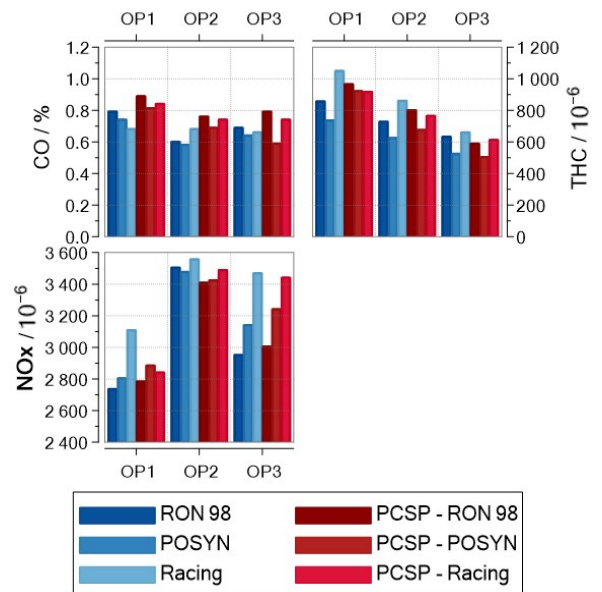


Fig.10 Influence of fuel and passive prechamber ignition

The slightly increased engine efficiency with the PCSP compared to the conventional spark plug can be exceeded only by the use of the advanced fuel formulations. Due to the fact, that the PCSP is not

optimized for the engine configuration and combustion design the use in combination with the advanced fuels has only minor effects. The main potential results from the fuel formulation.

As mentioned before the influence of changed combustion design and engine operation should not result in increased emissions. Therefore, it is important that the prechamber combustion does not show any negative effects on the gaseous and particle emissions. The biggest potential regarding emission formation results from the use of the POSYN fuel. The positive effects especially on THC and particle emissions was already discussed in references [2-3]. Due to issues with the measurements technique only the gaseous emissions are shown.

3.3 Advanced simulation analysis methodology

Considering the methodology described in the Section 2.3, OP1, OP2 and OP3 were calibrated in the 3D-CFD virtual test bench with respect to the

experiments. The investigated engine configuration through the numerical analysis corresponds to the configuration “Base setup” with reference to Tab. 1 (bore of 97 mm, a stroke to bore ratio of 0.835 and a compression ratio of 12.5). In the current section are reported the results for the operating point 6 000 r/min and 22 bar IMEP (OP3), which shows to be critical for mixture formation and therefore sensitive to knock onset.

Tab. 6 resumes the results with two different fuels (SP 98 and POSYN) comparing the measurements and the respective 3D-CFD simulation. The models of the two engine simulations showed in Tab. 6 differ only for the fuel definition, meaning that the caloric, the liquid properties (viscosity, surface tension, evaporation enthalpy and pressure of saturation), the laminar flame speed and the autoignition delay are different. No more parameters were adjusted in the two simulations.

Tab.6 Comparison of the results obtained with SP98 and POSYN at the test bench and the respective calibrated 3D-CFD simulation at 6000 rpm 22 bar IMEP (OP3)

Case description	Ignition point/ (° CA b. FTDC)	IMEP/bar	Indicated efficiency /%	Max. pressure/bar	Knock index/%	MFB 50/ (° CA a. FTDC)	MFB 90-10/ (° CA)	Temp. 40° CA b. FTDC/K	$\lambda_{@IP}$
Test bench SP 98	-10.5	22.5	37.5	85	Knock limit	22.1	29.2		1.003
Sim SP 98	-10.5	22.5	37.1	85	2.32	22.8	27.6	571	1.006
Test bench POSYN	-15.9	22.8	39.5	110	Knock limit	14.1	28.1		1.003
Sim POSYN	-16	23.3	38.8	110	3.95	15.7	25.7	552	1.008

For both fuels the simulations were regulated adjusting the ignition point exactly as the test bench. POSYN showed higher knock resistance and therefore the ignition point could be advanced up to 6° CA with respect to SP 98. The knock index was found for each fuel and it was taken into account as knock threshold for further investigated engine layouts just by means of 3D-CFD simulations. The knock index reported in Tab. 6 represents in the simulation the percentage amount of unburned gas, which are in self-ignition conditions, with respect to the overall unburned gas mass. The knock index values are different for each fuel and, based on some calibration results also for other operating points and engine configurations, the absolute value of it should be considered as a secondary reference value. On the

other hand, the most important parameter should be, for each fuel, the spark advance value which is responsible for an exponential growth of the knock index. The spark advance right before the exponential growth of the knock index is taken as knock-limit and it is found exactly aligned with the experimental ignition point, as shown in Tab. 6. The crank angle resolved curves of the knock index (or the percentage of mass in self ignition condition over the total mass of unburned gas), together with the burn rate are reported in Fig. 11 for the two fuels.

The burn rate and the centre of combustion are also quite accurately predicted by the simulations. In addition from Tab. 6, it can be highlighted the higher cooling power of POSYN compared to SP 98. POSYN led to 20 K lower in-cylinder temperature at

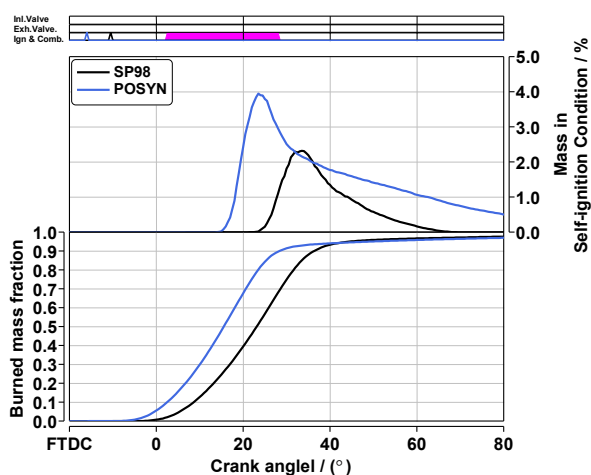


Fig. 11 Comparison of knock index and burn rate at 6 000 r/min and 22 bar IMEP for the two fuels

40°CA before firing top dead center, compared to SP 98. As discussed in reference [5-6], POSYN has higher evaporation enthalpy compared to SP 98, which contributes to lower down in-cylinder temperature and therefore increased knock resistance, but it has also a delayed start of evaporation and a narrow evaporation temperature window compared to SP 98. These differences are responsible for an overall not comparable mixture formation generated by the two fuels. The next analysis therefore, reports the different combustion development and knock behaviour of the two fuels considering the whole combustion chamber.

Fig. 12 pictures a normal combustion event triggered by a spark advance of 10.5° CA b. FTDC in case of SP 98, at 6 000 r/min and 22 bar IMEP. The measurements are taken close to the engine knock limit. The simulation shows the onset of some mass in self-ignition conditions (purple zones) between the exhaust valve and the liner. Nevertheless, the amount of the mass in critical conditions is not crucial and the flame front reaches soon the end-gas region (purple), preventing knock.

On the other hand, looking at Fig. 13, the same case is now performed with an earlier spark advance (16° CA b. FTDC), corresponding to the spark advance which triggers a normal combustion event for POSYN. SP 98 produces, in this conditions, an abnormal combustion as it can be seen from Fig. 13.

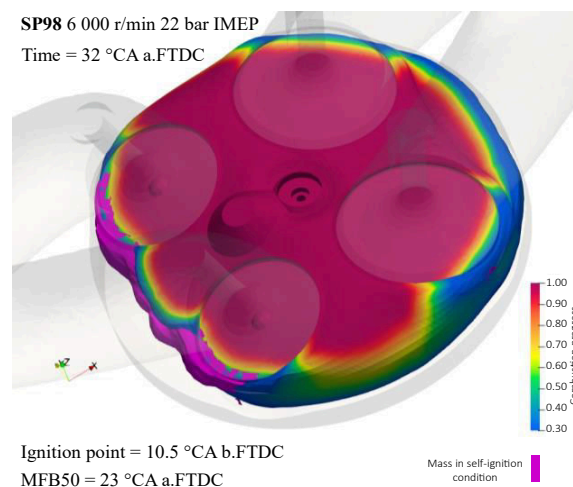


Fig.12 Combustion progression at 32° CA a.FTDC for SP98 (colorful scale) with respect to the mass in self ignition conditions (purple mass) at MFB 50 for a spark advance generating a normal combustion event

Here, the mass in self-ignition conditions distributes all over around the liner and, especially close to the intake valves. On top of that the flame front appears to be further from the end-gas which have self-ignition tendency.

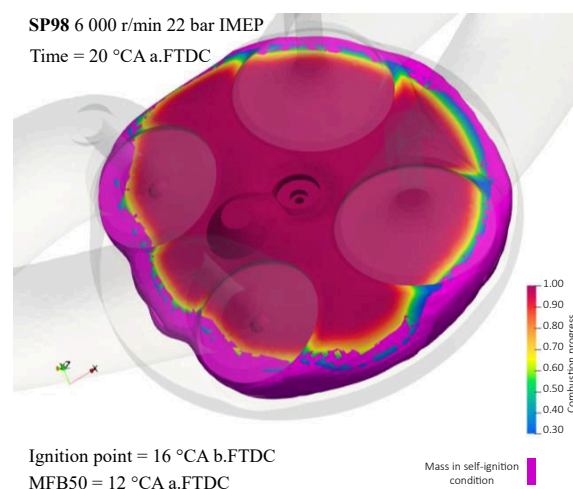


Fig. 13 Combustion progression at 20° CA a.FTDC for SP98 (colorful scale) with respect to the mass in self ignition conditions (purple mass) at MFB50 for a spark advance generating an abnormal combustion

The same ignition point is then investigated in case of POSYN in Fig. 14. Here the mass in self-ignition condition is clearly reduced with respect to SP 98, mostly because of the lower in-cylinder temperature.

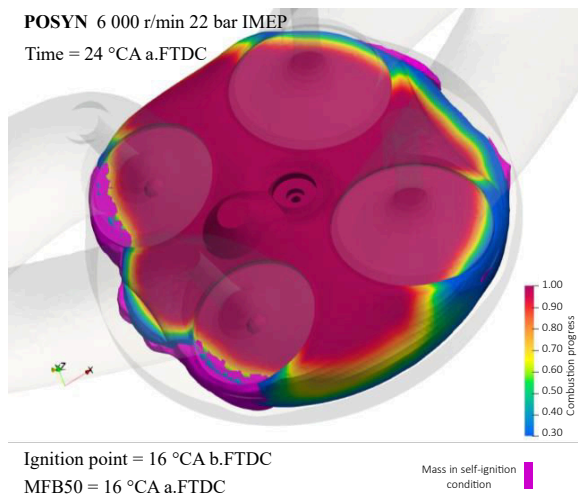


Fig. 14 Combustion progression at 24 °CA a.FTDC for POSYN (colorful scale) with respect to the mass in self ignition conditions (purple mass) at MFB 50 for a spark advance generating a normal combustion (earlier spark advance compared to SP 98)

Nevertheless, some critical regions can be identified close to the intake valves where the flame front distance from the gas in critical conditions is lower. This distribution is globally not dangerous for the engine or at the limit of knock, as shown also from the experiments.

Comparing MFB 50 and MFB 90 of the different cases, it can also be marked that SP98 burns faster than POSYN up to MFB 50, but POSYN accelerates the second part of the combustion (MFB 50–90). This trend was detailed explain in reference [5-6], analyzing the mixture formation in the simulation and it is essentially due to the different fuel evaporation behaviour. POSYN tends to have a delayed evaporation and therefore not an optimal start of mixture preparation. Later on, the few chemical species composing POSYN completes their evaporation earlier, allowing POSYN to cover the mixture formation timing gap with respect to SP 98 and exploiting the higher cooling power. The early the SOI for POSYN the higher the fuel potential to increase the engine resistance to knock and therefore the higher the indicated efficiency.

4 Conclusions

The requirements for CO₂ neutrality pose major challenges to the transportation sector. Regenerative fuels can make a significant contribution here, both for existing vehicles and for future combustion engines. In addition to the manufacturing paths for sustainable fuels, the efficiency of the combustion engine also plays an important role. Optimized fuel formulations, through degrees of freedom during production, can positively influence the combustion quality and thus increase engine efficiency. This can be exploited by co-optimizing eFuel formulation and the internal combustion engine.

For this purpose, potentials were experimentally investigated in the present work by means of an advanced combustion design. In addition to two further developed single-cylinder engines with increased compression ratio and optimized stroke/bore ratio, initial potentials were also identified via the fuel and a passive prechamber ignition system. It was shown that the fuel already outperforms the improved combustion quality and the increased efficiency with the prechamber ignition. The non-specifically designed prechamber has shown minor impact with advanced fuels.

Simulation models and methods were developed in order to perform an efficient and fast evaluation of the optimization possibilities of the combustion processes in conjunction with the fuel. The paper describes different solutions to implement and improve the use of synthetic fuels in internal combustion engines, also highlighting the differences and the potential with respect to a conventional gasoline. The methodology for the fuel comparison has been also shown, considering the essential exchange between experiments and virtual development. A further step will be the test of this procedure to optimize the use of synthetic fuels in other engine geometries and the comparison of the 3D-CFD simulation results with optical measurement of the knock onset in the combustion chamber.

References:

- [1] United Nations. The Paris Agreement[Z]. 2015. http://unfccc.int/paris_agreement/items/9485.php2019.
- [2] ALBRECHT M, DEEG H-P, SCHWARZENTHAL D, *et al.* Investigations of the emissions of fuels with different compositions and renewable fuel components in a GDI engine [J]. SAE Technical Paper, 2020-01-0285. DOI: <https://doi.org/10.4271/2020-01-0285>.
- [3] KULZER A C, DEEG H-P, VILLFORTH J, *et al.* Sustainable mobility using fuels with pathways to low emissions [J]. SAE Int J Advances & Curr Prac, 2020, 2(4): 1870. DOI: <https://doi.org/10.4271/2020-01-0345>.
- [4] VILLFORTH J, KULZER A C, WEIBHAAR A, *et al.* The influence of eFuel formulation on post oxidation and cold start emissions [J]. SAE Technical Paper, 2021-01-0632. DOI: <https://doi.org/10.4271/2021-01-0632>.
- [5] VILLFORTH J, KULZER A C, DEEG H-P, *et al.* Methods to investigate the importance of eFuel properties for enhanced emission and mixture formation [J]. SAE Technical paper, 2021-24-0017. DOI: <https://doi.org/10.4271/2021-24-0017>.
- [6] ROSSI E, HUMMEL S, CUPO A, *et al.* Experimental and numerical investigation for improved mixture formation of an eFuel compared to a standard gasoline [J]. SAE Technical Paper, 2021-24-0019. DOI: <https://doi.org/10.4271/2021-24-0019>.
- [7] CHIODI M. An innovative 3D-CFD-approach towards virtual development of internal combustion engines [D]. Stuttgart: University of Stuttgart, 2010.
- [8] CUPO F. Modeling of real fuels and knock occurrence for an effective 3D-CFD virtual engine development [D]. Stuttgart: University of Stuttgart, 2021.
- [9] MEHL M, PITZ W J, WESTBROOK C K, *et al.* Kinetic modeling of gasoline surrogate components and mixtures under engine conditions[J]. Proceedings of the Combustion Institute, 2011, 33(1): 193.
- [10] WENTSCH M. Analysis of injection processes in an innovative 3D-CFD tool for the simulation of internal combustion engines [D]. Stuttgart: University of Stuttgart, 2018.
- [11] VACCA A, HUMMEL S, MÜLLER K, *et al.* Virtual development of injector spray targeting by coupling 3D-CFD simulations with optical investigations [J]. SAE Technical Paper, 2020-01-1157. DOI: <https://doi.org/10.4271/2020-01-1157>.